Signature of microphysics on spatial rainfall statistics

A. Parodi,[1] E. Foufoula-Georgiou,[2] and K. Emanuel[3]

Received 28 September 2010; revised 21 March 2011; accepted 28 April 2011; published 30 July 2011.

[1] Previous studies have suggested that the statistical multiscale structure of rainfall can be parameterized in terms of thermodynamic descriptors of the storm environment, and such dependence has been successfully implemented in downscaling applications. In this paper we suggest that it is possible to adopt the raindrop terminal velocity as a physical parameter to explain to a large degree the statistical variability of convective rainfall over a range of scales. We examine this assertion by analysis of high-resolution simulations of an atmosphere in radiative-convective equilibrium performed using the Weather Research and Forecasting (WRF) model and prescribing different rain terminal velocity settings corresponding to small, slowly falling drops and large, quickly falling drops, respectively. The analysis has focused on the study of the dependence of some basic statistics of rainfall fields (probability distribution of convective rain cell areas, power spectra, and multiscale statistics of rainfall intensity) on the raindrop terminal velocity by using a well-documented and widely used atmospheric model. Possible applications of our results include downscaling of rainfall satellite measurements, conditional on limited microphysical information from dual-frequency spaceborne radars, and conversion of radar reflectivity to rain rate, conditional on drop size distribution inferred from the scaling parameters of the reflectivity fields.

Citation: Parodi, A., E. Foufoula-Georgiou, and K. Emanuel (2011), Signature of microphysics on spatial rainfall statistics, *J. Geophys. Res.*, *116*, D14119, doi:10.1029/2010JD015124.

1. Introduction

[2] Understanding the space-time rainfall variability over a range of scales (from seconds to several days in time and meters to several kilometers in space) has been the subject of intensive research over the past two decades [*Georgakakos and Cramer*, 1994; *Lovejoy and Scherzter*, 2006; *Lovejoy and Allaire*, 2008; *Olsson and Berndtsson*, 1993; *Over and Gupta*, 1994]. Emphasis has been placed on concise parameterization of this variability across a range of scales exploring concepts of scale invariance and statistical renormalization [*Gupta and Waymire*, 1996; *Lovejoy and Schertzer*, 1985; *Kumar and Foufoula-Georgiou*, 1993; *Venugopal and Foufoula-Georgiou*, 1996; *Ferraris et al.*, 2003]. One issue that has not been adequately addressed is the fundamental understanding of what key physical parameters of the storm environment explain most of the observed statistical variability of rainfall. Along this direction, *Over and Gupta* [1994] examined large-scale predictors of this variability, while *Perica and Foufoula-Georgiou* [1996] focused on the storm thermodynamic environment. In that latter study, the Convective Available Potential Energy (CAPE) ahead of the storm was empirically found to relate to the scaling properties of spatial rainfall. Under an energy cascading interpretation of the spatial scaling in rainfall intensity, the above finding was interpreted as saying that the larger the instability ahead of the storm, the more turbulent the storm environment and the larger the scale-to-scale change of spatial variability in rainfall fields. In this paper we pose the question as to whether the relation of the spatial rainfall multiscale variability and physical observables can be shown more rigorously in a physical rather than empirical or statistical context.

[3] Along these lines, our idea is to evaluate if, according to the moist convective scaling theory of *Parodi and Emanuel* [2009], it is possible to adopt the raindrop terminal velocity (or a related microphysical parameter) to define a relation between physical and statistical parameters of precipitation. We test this hypothesis by analysis of high-resolution simulations of an atmosphere in radiative-convective equilibrium performed using the Weather Research and Forecasting (WRF) model and prescribing different rain terminal velocity settings corresponding to small, slowly falling drops and large, quickly falling drops, respectively. This study is specifically focused on an investigation of the dependence of some basic statistics of rainfall fields (probability distribution of convective rain cell areas, power spectra and multifractal rain intensity statistics) on the raindrop terminal velocity in deep moist convective environments.

2. Experimental Design

[4] The deep moist convective scenarios here considered refer to the results of *Parodi and Emanuel* [2009], who

[1]CIMA Research Foundation, Savona, Italy.
[2]Department of Civil Engineering, Saint Anthony Falls Laboratory, University of Minnesota, Minneapolis, Minnesota, USA.
[3]Program in Atmospheres, Oceans, and Climate, Massachusetts Institute of Technology, Cambridge, Massachusetts, USA.

0148-0227/11/2010JD015124

performed high-resolution simulations of an atmosphere in radiative-convective equilibrium using the Weather Research and Forecasting (WRF) model (version 2.2), which is a fully compressible, nonhydrostatic, scalar-variable conserving cloud-resolving model [*Skamarock et al.*, 2005]. There is a long-standing tradition in the literature of using the radiative-convective equilibrium scenario to study fundamental properties of deep moist convective processes [*Emanuel*, 1994]. Indeed, the radiative-convective equilibrium scenario shares many characteristics with more realistic deep moist convection scenarios and presents a simple and useful framework within which to tackle new research issues such as that of linking microphysical parameter(s) to rainfall stochastic characterization. A state of moist radiative-convective equilibrium corresponds to an atmospheric state in which the divergence of the net vertical radiative flux is balanced by the convergence of the vertical flux of enthalpy in convective clouds, apart for a thin boundary layer close to the surface, where dry turbulence would be responsible for the flux. Even though it is well known that such a radiative-convective state is not necessarily stable to large-scale perturbations, this does not diminish its importance for the study of fundamental physical processes of dry and moist convection. The canonical problem of radiative-dry convective equilibrium was first formulated by *Prandtl* [1910, 1925]. Important studies of precipitating radiative-convective equilibrium include those of *Held et al.* [1993], *Islam et al.* [1993], *Robe and Emanuel* [1996], *Tompkins and Craig* [1998a, 1998b], *Robe and Emanuel* [2001], *Pauluis and Held* [2002a, 2002b], *Wu* [2002], *Grabowski* [2003], and *Nolan et al.* [2007].

[5] As with much of the published literature, in this study the radiative-convective equilibrium scenario is represented by a doubly periodic domain capped by a stable layer that represents the stratosphere. The WRF model is run on a domain of size L = 200 km: a uniform horizontal spatial resolution of 2 km is adopted, while the vertical grid spacing stretches gradually from 100 m near the bottom boundary to 500 m near the top one.

[6] A constant cooling rate Q_{rad} is applied over the depth of the troposphere ($0 < z < 15$ km), while above it a sponge layer relaxes the scalar state variables back to observed stratospheric profiles: the results of this paper refer to $Q_{\mathrm{rad}} = -4$ K/d. The turbulence parameterization is based on a 1.5 order large eddy simulation (LES)-like approach [*Mellor and Yamada*, 1974].

[7] The initial atmosphere is horizontally homogeneous, with a vertical temperature profile similar to Jordan's sounding [*Jordan*, 1958]. The atmosphere is made unstable by the aforementioned constant radiative cooling from the surface to the tropopause coupled with surface enthalpy fluxes, from an ocean with constant temperature T_S = 300.15 K. Spatially random temperature perturbations in the lower atmosphere ($0 < z < 2500$ m) are applied in the initial condition to trigger convection. The perturbation values are in the range −0.5–0.5 K and do not produce domain-averaged heating.

[8] *Parodi and Emanuel* [2009] characterized the velocity and buoyancy scales for moist convection in statistical equilibrium and showed that buoyancy and velocity scales at equilibrium depend on the terminal velocity of raindrops. Subsequently, *Parodi and Emanuel* [2009] presented a novel theory explaining this behavior and evaluated it in the context of the numerical results provided by the WRF model.

[9] The microphysics are parameterized according to the warm rain scheme of *Kessler* [1969], whose physical and numerical formulation has been modified in order to allow one to prescribe values of the precipitation terminal velocity, V_T, that are constant and independent of the hydrometeor size distribution [*Parodi and Emanuel*, 2009]. This scheme, fully evaluated in the aforementioned reference, allows one to control in a simple and efficient way one of the influences exerted by microphysics on moist convection. In this context, small terminal velocity values will mimic the predominance of small and light raindrops, while large values will be associated with the presence of larger and heavier raindrops: indeed at equilibrium the imposed terminal velocity results in average drop sizes and drop size distribution (DSD), in good agreement with expected values (see *Pruppacher and Klett* [1997], *Straka* [2009], and Appendix A for details). This confirms that in the numerical simulations the computed drop size distributions are within a physically reasonable range. It is worth emphasizing that the results obtained using this microphysics setting are in complete agreement with those presented by *Grabowski* [2003]. Specifically, the thermodynamical structure of the precipitating radiative-convective equilibrium obtained by *Parodi and Emanuel* [2009] for low (high) V_T values is consistent with that presented by *Grabowski* [2003] for small (large) cloud and precipitation particles. Along similar lines, a number of modeling and observational studies have highlighted the important role of microphysics (namely the DSD) in determining the spatiotemporal properties of deep moist convective processes in different weather scenarios [*Brawn and Upton*, 2008; *Caracciolo et al.*, 2006, 2008; *Chumchean et al.*, 2008; *Georgakakos and Krajewski*, 1996; *Gilmore et al.*, 2004; *Grubisic et al.*, 2005; *Hong et al.*, 2009; *Liu and Moncrieff*, 2007]. Among others, *Caracciolo et al.* [2008] pointed out the crucial role of the DSD parameters for understanding the physics of rainfall formation processes and for discriminating between different rainfall patterns and spatiotemporal properties (e.g., stratiform and convective), while *Georgakakos and Krajewski* [1996] determined the statistical-microphysical causes of rainfall variability in the tropics by analyzing the links between statistical theories of rainfall phenomenology and kinematic-microphysical theories of rainfall production mechanisms.

3. Analysis of the Dependence of the Properties of Convection on the Terminal Velocity of Raindrops

3.1. Scaling of Cell Size Statistics With Terminal Velocity

[10] On the basis of *Parodi and Emanuel* [2009] and *von Hardenberg et al.* [2003], a simple algorithm for extracting rainfall convective cells from each spatial frame field has been applied. This algorithm allows one to retain rainfall convective cells above a prescribed rainfall intensity threshold, R_s, in order to compute such related statistics as the mean cell size, the coefficient of variation of the cell size, and a few other metrics. According to this algorithm, a local maximum in the rainfall intensity field is identified as a

pixel value that has an intensity exceeding the threshold and is larger than any of its 20 nearest neighbors. Each maximum represents the center of a cell. The algorithm traces progressively lower contour levels around each cell center. The extraction procedure here adopted is affected by different sources of uncertainty but the results are robust to changing parameters in the algorithm for cell identification and comparable to similar techniques for cell extraction [*Steiner et al.*, 1995]. The horizontal extent of each rain cell, A_C, is provided by the connected region around each cell center that has intensity larger than 0.5 mm h^{-1}. Having defined the cells that way, the mean cell size, $\langle A_C \rangle$, and the coefficient of variation of the cell size are computed over the ensemble of spatial frames (200 km by 200 km at pixel resolution of 2 km) and over a period of 5 days (with a temporal step of 30 mins) in radiative-convective equilibrium.

[11] The results presented in the following sections pertain to the values of the raindrop terminal velocity in the range $0 < V_T < 15$ m s^{-1} and to $R_s = 2$ mm h^{-1}: the size distribution of the extracted cells is comparable to the size distribution of cells in observed precipitating systems [*Gryschka et al.*, 2008].

[12] Interestingly, the mean cell size, $\langle A_C \rangle$ (Figure 1a), when plotted against the raindrop terminal velocity in a log-log scale, exhibits two distinct regimes for V_T values in the ranges 1–5 m s^{-1} (denoted as region I) and 6–15 m s^{-1} (denoted as region II). One could argue that a log-log linear approximation is possible in both ranges, suggesting a potential scaling behavior of mean rain cell area with V_T, expressed as a power law:

$$\langle A_C \rangle = kV_T^{\gamma}, \tag{1}$$

with the coefficients k and γ given as

$$k = 130, \gamma = -0.71, 1 < V_T \leq 5 \text{ m/s} \tag{2}$$

$$k = 69, \gamma = -0.32, 5 < V_T < 15 \text{ m/s}. \tag{3}$$

[13] It was found that the exponents of −0.7 for smaller terminal velocities and −0.3 for larger velocities are robust to the definition of rain cell, that is, they remain invariant for different thresholds defining the cells (i.e., R_s = 5 mm h^{-1}, not shown here). It is observed, from the above power law scaling, that in the range 1–5 m s^{-1}, doubling the value of V_T results in a mean rain cell size reduction by a factor ≈0.6 ($2^{-0.7}$), while for $V_T > 6$ m s^{-1} the decrease is slower, i.e., by a factor ≈0.8 ($2^{-0.3}$).

[14] While the behavior of the mean cell size as a function of terminal velocity is interesting, there is a great deal of variability in the size of the cells (see Figure 1b for the frequency histograms of cell sizes for different V_T values). Thus characterizing at least the variance (if not higher-order statistical moments) is essential. In that spirit, the normalized variability, that is, the coefficient of variation (CV) is computed and plotted against V_T (Figure 2). Once again, two different regimes seem to arise: for low V_T values the coefficient of variation increases rapidly (region I), while for higher V_T values (above 6 m s^{-1}, region II) it becomes asymptotic to a value around 0.85. The power law scaling of the mean cell size $\langle A_C \rangle$ with V_T and the increase (constant value) of CV for V_T smaller (greater) than 5 m s^{-1} suggests that the dependence of cell statistics on V_T is simple scaling for large velocities and multiscaling for small velocities (see Appendix B for details). Simple scaling implies that a single scaling exponent can describe how the shape of the whole probability distribution of cell area sizes changes as the terminal velocity (serving as the scale parameter here) changes, while multiscaling implies that this relationship is more complicated and needs more than one parameter to be characterized. Putting it more simply, the results here indicate that for small V_T values, the standard deviation of the cell areas grows proportionally faster than the mean cell area (CV increases with V_T), while it grows at almost the same rate for larger V_T values (CV constant with V_T). The implications of this rich statistical scaling structure being explained by a single microphysical variable, such as terminal velocity V_T, is worth exploring on physical, rather than empirical grounds, and this will be discussed in the following section.

3.2. Relationship Between Total Mass Flux, Updraft Velocity, and Cell Size

[15] A physical understanding of the mean cell size scaling with terminal velocity can be provided by combining the moist convection theory of *Parodi and Emanuel* [2009] with some ideas about the scaling of the total mass flux M_U. The *Parodi and Emanuel* [2009] theory allows one to estimate a scale for the updraft vertical velocity, $w_{updraft}$, for each value of the raindrop terminal velocity on the basis of a quadratic moist scaling theory:

$$cV_T w_{\text{updraft}}^2 + bq^* w_{\text{updraft}} - acs' V_T - bd = 0, \tag{4}$$

where q^* is a characteristic difference between the specific humidity in and outside the cloud, s' represents fluctuations of moist entropy in the boundary layer, and a, b, c and d are constants. The values of the constants a, b, c, d and scales q^* and s' are provided in Tables 1 and 2 (see also *Parodi and Emanuel* [2009]). On the basis of equation (4), w_{updraft} grows with V_T in the range 1–5 m s^{-1}, while for higher V_T values it tends to an asymptotic value (see Figure 3a). Furthermore, the following expression holds for the total mass flux M_U [*Emanuel and Bister*, 1996], where S_P is the static stability function:

$$M_U = \frac{Q_{\text{rad}}}{S_p}. \tag{5}$$

The static stability function can be expressed as

$$S_p = \frac{(\Gamma_d - \Gamma)}{\rho g}, \tag{6}$$

where Γ is the actual temperature lapse rate, Γ_d is the dry adiabatic lapse rate, ρ is the air density and g the acceleration of gravity. The product of the vertical velocity w_{updraft} and the total cell area A_c should be equal to the mass flux M_U, provided that downdrafts are neglected. Consequently, the mean cell size $\langle A_c \rangle$ relates to the parameter $\alpha \equiv M_U / w_{\text{updraft}}$ with the relationship (derived from relationships (4) and (1)):

$$\langle A_C \rangle = k \left[\frac{b(d\alpha^2 - q^* M_U \alpha)}{cM_U - acs'\alpha^2} \right]^{\gamma}, \tag{7}$$

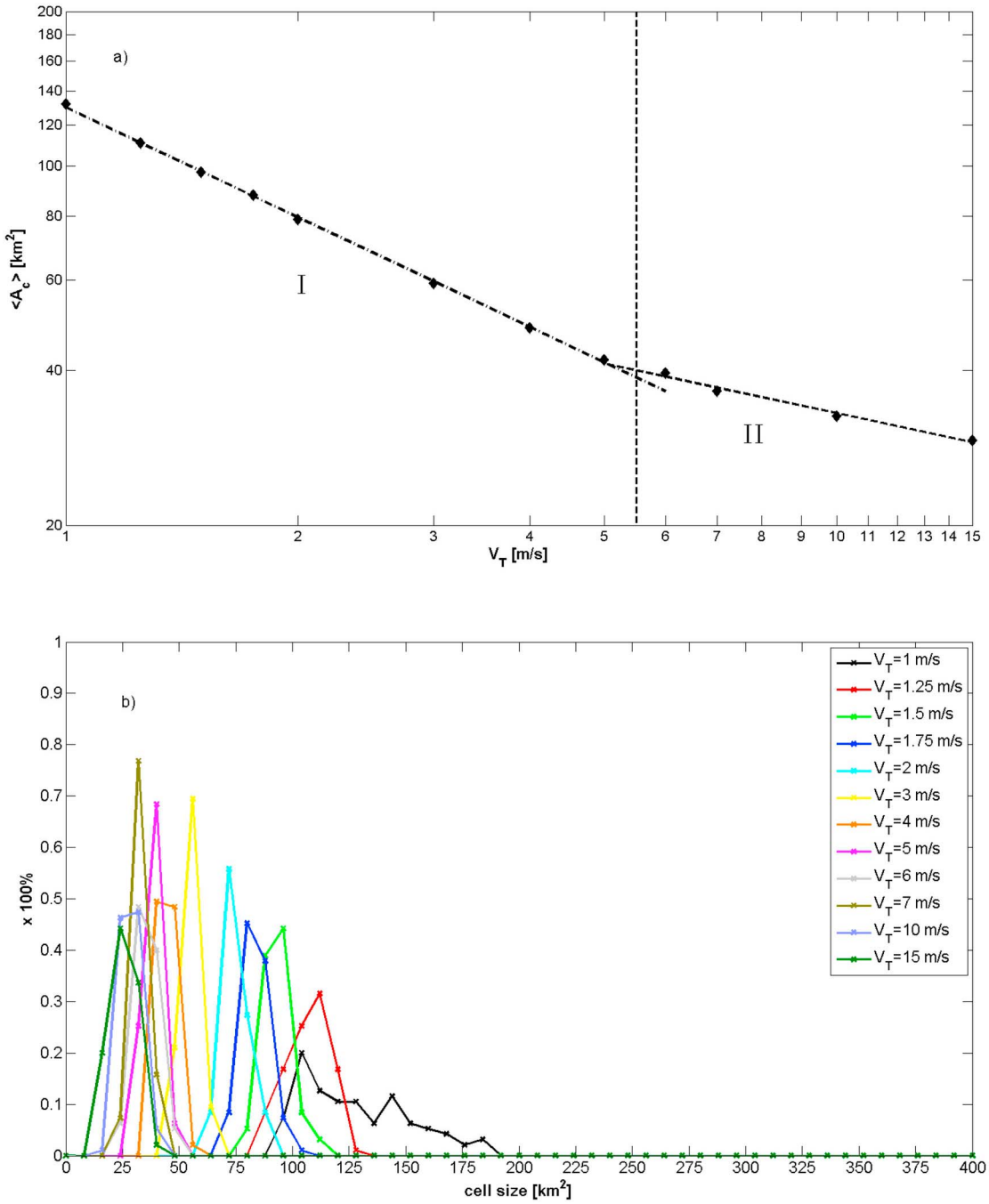

Figure 1. (a) Mean cell size, $\langle A_c \rangle$, versus the raindrop terminal velocity V_T on log-log axes (threshold for definition of cells is $R_s = 2$ mm h^{-1}). The dash-dotted line corresponds to the power law $\langle A_c \rangle = kV_T\gamma$ (equation (1)) in the range 1–5 m s^{-1} (region I), while the dashed line corresponds to the power law in the range 6–15 m s^{-1} (region II). (b) Frequency histograms of the cell size A_C for different values of the raindrop terminal V_T.

where $\gamma = -0.7$ for $\langle A_C \rangle \gtrsim 40$ km^2 or $V_T \leq 5$ m s^{-1} and $\gamma = -0.3$ for $\langle A_C \rangle \lesssim 40$ km^2 or $V_T > 5$ m s^{-1}. This relationship, displayed in Figure 3b emphasizes the dependence of a statistical expression of rainfall spatial variability (mean rain cell area, $\langle A_C \rangle$) to a physical parameter of the storm environment, namely α, which can potentially be resolved from observable quantities (e.g., as recently investigated by *Tao et al.* [2006], *Blossey et al.* [2007], *Feldman et al.* [2008], and *Robin et al.* [2008]).

4. Power Spectral Analysis of Accumulated Rainfall Patterns

[16] Power spectral analysis represents a relevant tool to examine the ability of a numerical model to represent the

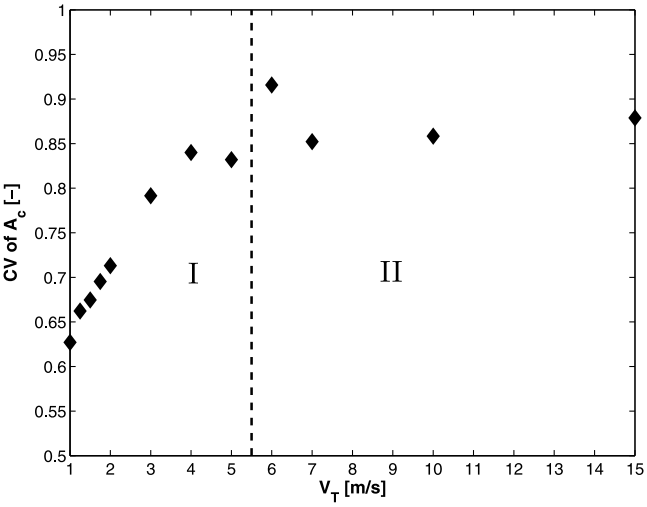

Figure 2. Coefficient of variation of the cell size A_c versus the raindrop terminal velocity V_T (threshold $R_s = 2$ mm h^{-1}). Region I and region II are identified in the plot.

energy cascading from energy-containing eddies down to dissipative eddies. The power spectrum is also useful in determining how accurately features of various wavelengths are resolved and to quantify the resolution limits and the effectiveness of the dissipation mechanisms of a numerical weather prediction model [*Skamarock*, 2004]. In this framework, a power spectral analysis of the accumulated rainfall fields, over durations of d = 3, 6, 12, and 24 h, and over a period of 5 days in radiative-convective equilibrium, is presented. As a term of reference, a few snapshots of the 3-hourly and daily accumulated rainfall fields for $V_T = 1$ and 10 m s^{-1}, are presented in Figure 4. When the terminal velocity is larger, the convective cells are stronger, isolated and smaller in size (larger CV as documented earlier), while in the case of the low V_T experiments, the rainfall field exhibits a more spatially uniform pattern (lower CV values but drastically changing as the value of V_T increases), reminiscent of a Rayleigh-Benard organization.

[17] Figures 5 and 6 show the 2-D isotropic radially averaged power spectra for the d = 3 h and d = 24 h accumulated rainfall fields, respectively. The computed spectra are consistent with other results obtained for precipitating radiative-convective equilibrium [*Shutts and Gray*, 2007]. Both the 3-hourly and daily accumulated rainfall fields exhibit a power law scaling regime over a range of length scales which depends on the value of the vertical velocity. For lower raindrop velocities, the energy dissipation is occurring more actively (steeper spectral slope) and over a larger range of scales. On the contrary, for very large terminal velocities, the rainfall intensity fields approach an almost random white noise structure. Larger V_T is expected to result in precipitation fields which have a smaller spectral slope simply because the "energy" in these systems is almost equally distributed over a wide range of scales (the spectrum is flatter). Furthermore, it is noted that especially for increasing duration d, a well-defined peak in the power spectra appears at a scale of the order of 10–20 km (Figure 7). This peak arises from the fact that the model setting introduces a time invariant large-scale forcing contribution which imposes a characteristic scale in the accumulated rainfall fields (this scale however is larger than the largest cells we evaluate in this study (see Figure 1b) and thus does not restrict the interpretation of our results).

Table 1. Values of Parameters a, b, c, and d for the Quadratic Moist Scaling Theory[a]

Parameter	Value
a (K^{-1})	0.89
b (m^2 s^{-2})	3.46e + 3
c	2.817
d (kg/kg m s^{-1})	0.017

[a]*Parodi and Emanuel* [2009].

Table 2. Scales for the Definition of the Moist Scaling Theory[a]

V_T (m s^{-1})	q^* (kg/kg)	s' J/(kg K)
1	5.65E-03	19.73
1.25	5.73E-03	20.12
1.5	5.98E-03	20.72
1.75	5.90E-03	21.39
2	6.11E-03	21.95
3	6.54E-03	23.39
4	6.86E-03	24.19
5	7.10E-03	24.99
6	7.27E-03	26.07
7	7.70E-03	25.76
10	8.31E-03	26.22
15	9.10E-03	26.27

[a]*Parodi and Emanuel* [2009].

[18] Spectral slopes were estimated from the individual spectra of each simulated field via a least squares log-log linear fit over the scale range of 5–15 km with values comparable to those reported in the literature for real rainfall fields [*Harris et al.*, 2001; *Mandapaka et al.*, 2009; *Menabde et al.*, 1997; *Nykanen and Harris*, 2003]. The results displayed in Figure 8 show that the accumulated rainfall fields exhibit a robust power spectral slope independent of duration and that this slope strongly depends on V_T for V_T less than approximately 5 m s^{-1}. Given the relationship between V_T and the updraft velocity (equation (4) and Figure 3a) the results of Figure 9 can be interpreted in terms of the dependence of the power spectral slope on the updraft velocity scale: the "smoother" or more correlated the accumulated rainfall fields (larger spectral slopes), the lower the values of w_{updraft}, while the opposite is true for the less correlated ("rougher" with isolated convective cells) accumulated rainfall fields.

[19] The invariant character of the relationship between the spectral slope and terminal velocity to temporal accumulation within 3–24 h means that for precipitating radiative-convective equilibrium, larger temporal accumulations might be used to infer statistical properties of shorter time accumulations, provided that some homogeneity exists in the average microphysical properties as the storm evolves and in the large-scale forcing within those accumulation periods.

5. Subgrid-Scale Rainfall Variability and Physically Based Statistical Downscaling

[20] In the previous section we only characterized the size of the cells but not their intensity. In this section we perform a multiscaling analysis of rainfall intensities akin to that of *Kumar and Foufoula-Georgiou* [1993] and *Perica and Foufoula-Georgiou* [1996].

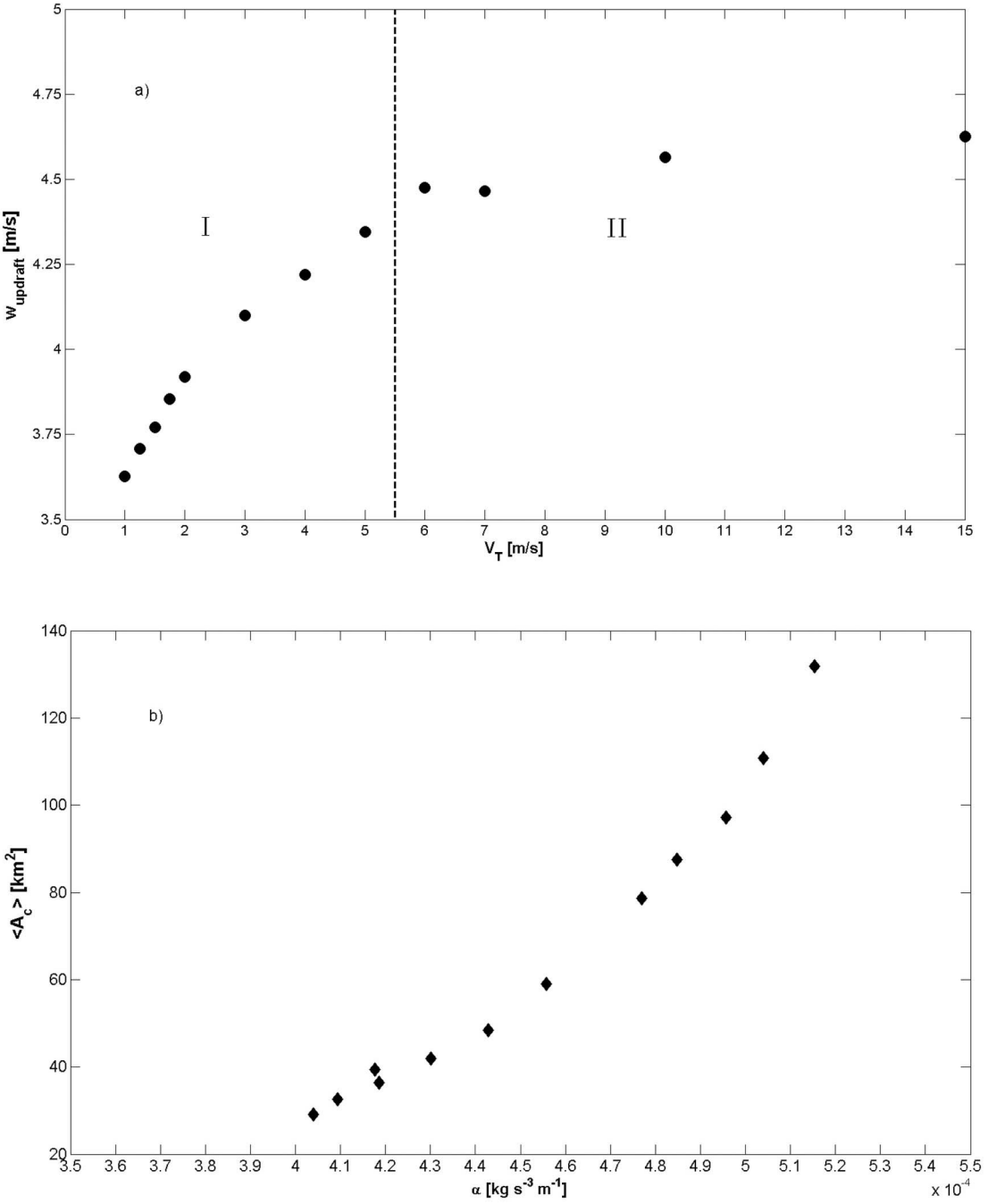

Figure 3. (a) Updraft velocity scale, w_{updraft}, as a function of the raindrop terminal velocity V_T, provided by the *Parodi and Emanuel* [2009] theory (see equation (4)). Region I and region II are identified in the plot. (b) Dependence of the mean cell area $\langle A_c \rangle$ on the parameter $\alpha \equiv \frac{M_U}{w_{\text{updraft}}}$, where M_U is the total mass flux. The analytical expression of the $\langle A_c \rangle$ versus α is given in equation (7).

[21] Through the analysis of numerous mesoscale convective storms, *Perica and Foufoula-Georgiou* [1996] found that the standardized rainfall fluctuations, namely, the rainfall fluctuations divided by their corresponding- scale average rainfall intensities, showed simple scaling between the scales of 4 × 4 and 64 × 64 km^2. On the basis of this result, a spatial downscaling scheme was developed. The precipitation fluctuations were defined via a 2-D Haar wavelet transform in dyadic scale. The decomposition of the spatial rainfall fields is orthogonal and requires three directional components (one in each horizontal, vertical and diagonal directions of the planar 2-D rainfall image). *Perica and Foufoula-Georgiou*

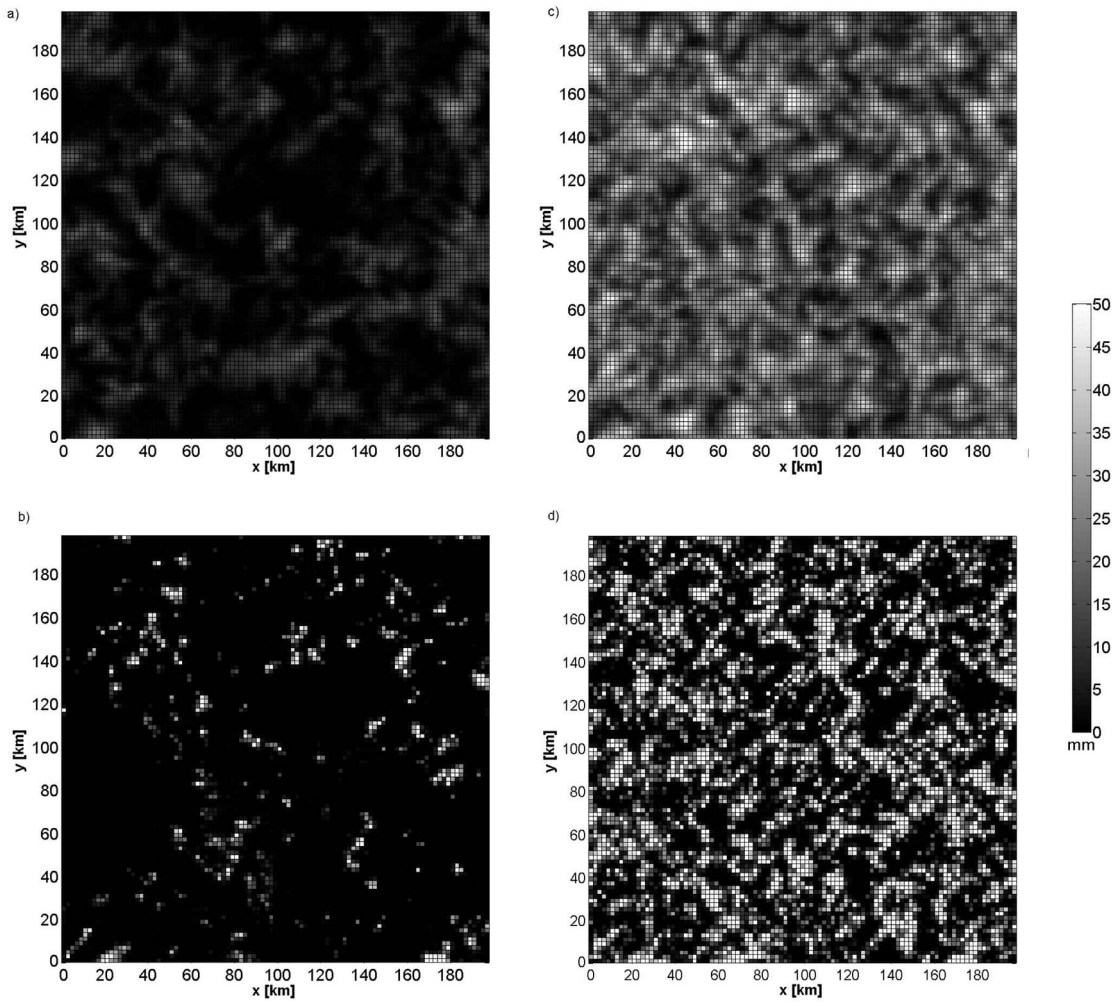

Figure 4. Frames of the 3-hourly accumulated rainfall field for (a) $V_T = 1$ m s^{-1} and (b) $V_T = 10$ m s^{-1}. Frames of the daily accumulated rainfall field for (c) $V_T = 1$ m s^{-1} and (d) $V_T = 10$ m s^{-1}.

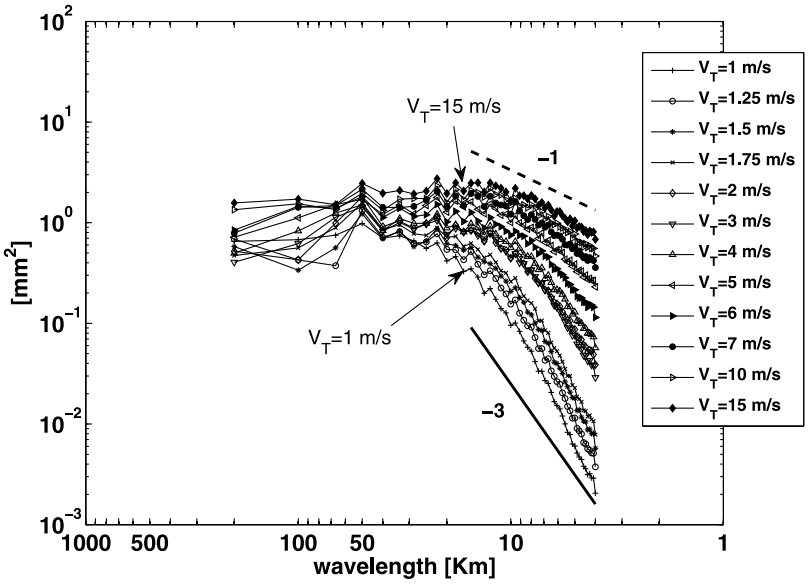

Figure 5. Power spectrum of the $d = 3$ h accumulated rainfall field for V_T values in the range 1–15 m s^{-1}. Characteristic spectral slopes equal to −1 and −3 are shown.

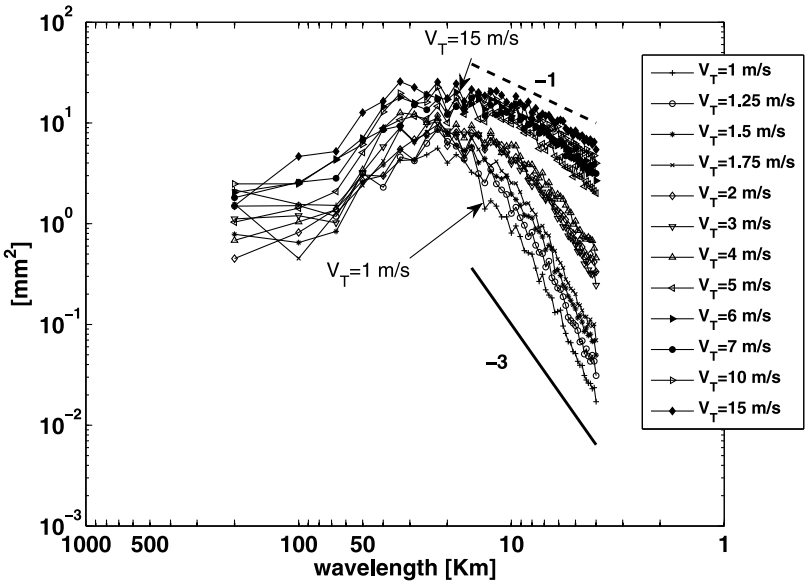

Figure 6. Same as Figure 5 but for d = 24 h.

[1996] demonstrated that the average, H, of the three directional scaling exponents H_i (where i = 1, 2, 3 is the horizontal, vertical and diagonal directions, respectively) can be related to the CAPE, hence providing an opportunity to relate the downscaling process to precipitation physics.

[22] Along the same lines, in this study we test, and subsequently quantify, the degree to which the directionally averaged downscaling coefficient H is related to the raindrop terminal velocity V_T. The analysis is performed for the accumulated rainfall fields corresponding to duration d = 3, 6, 12, and 24 h: the relationship of H with V_T is evaluated in the range $1 < V_T < 5$ m s^{-1} where cell statistics exhibit a multiscaling dependence on V_T. Figure 10 suggests that H is strongly dependent on V_T for the accumulated rainfall fields corresponding to d = 6, 12, and 24 h, while the dependence is weaker for d = 3 h. The coefficient of determination, R^2, is around 0.9 for d = 6, 12, and 24 h, and the value of H varies between 0.2 and 0.5 as V_T increases from 1 to 5 m s^{-1}. For duration d = 3 h the value of H remains almost constant and approximately equal to 0.1. This is consistent with our expectations; the larger the value of V_T the smaller the spatial persistence of the rainfall field (value of 0.5 would correspond to a Brownian surface). On the contrary, smaller values of V_T imprint a persistence on the multiscale statistics of rainfall as evidenced by the lower values of H in Figure 10 (coincidentally, *Perica and Foufoula-Georgiou* [1996] had reported values of H in the order of 0.3–0.5 for midlatitude convective storms). This finding supports the underlying

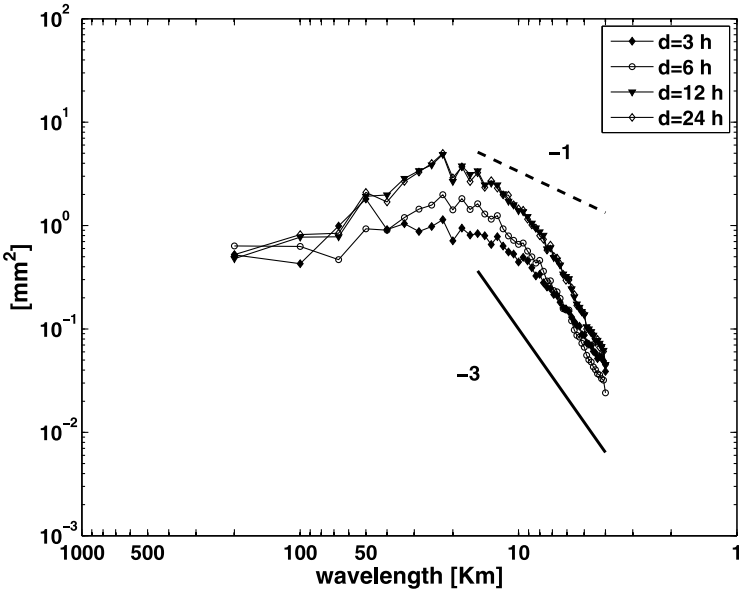

Figure 7. Power spectrum of 2-D rainfall fields for accumulation over durations d = 3, 6, 12, and 24 h and V_T = 2 m s^{-1}.Characteristic spectral slopes equal to −1 and −3 are shown.

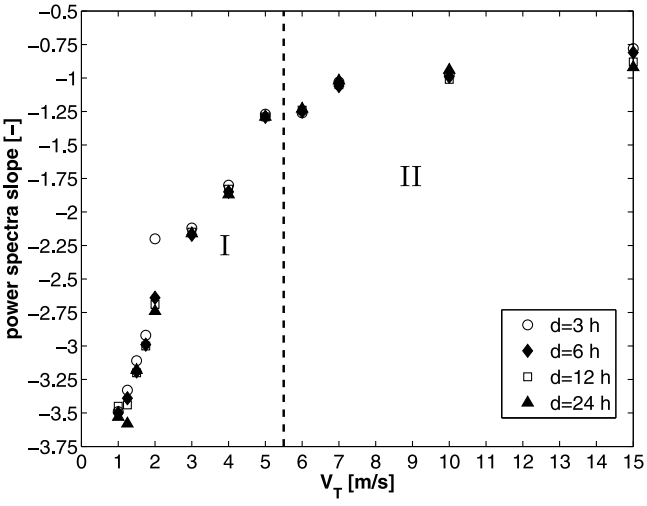

Figure 8. Accumulated rainfall spectral slope versus V_T (d = 3, 6, 12, and 24 h). Region I and region II are identified in the plot.

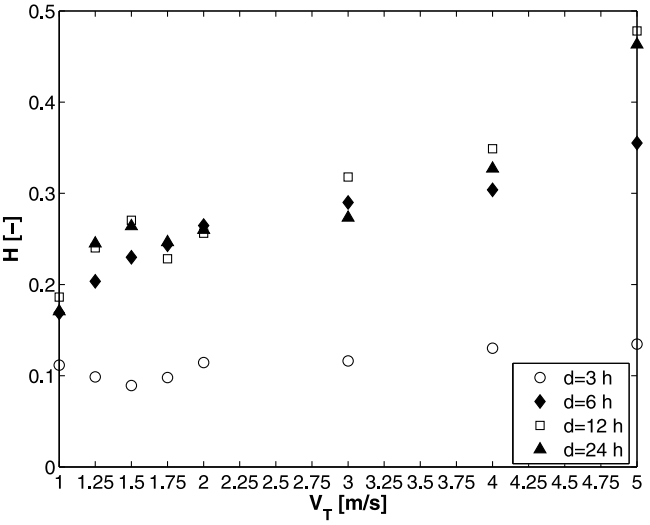

Figure 10. Variation of the downscaling parameter H versus V_T (d = 3, 6, 12, and 24 h).

premise of this study that identifies microphysics, parameterized here in terms of terminal velocity V_T, as explaining the statistical variability of convective rainfall over a range of scales for the deep moist convective scenario here examined.

6. Application of Results

[23] We envision that applications of the results presented in this study can be explored in two main directions. The first direction of applications relates to the statistical downscaling of precipitation fields, conditional on independently inferred, or directly observed, microphysical properties of the storm environment. Often, microphysical characteristics of storms are related to classified weather types [e.g., *Bradley and Smith*, 1994; *Frei and Schar*, 1998; *Rudari et al.*, 2005; *Molini et al.*, 2009; *Vrac and Yiou*, 2010]. For example, *Waldvogel* [1974], *Zawadski et al.* [1994], *Cifelli et al.* [2000], and *Caracciolo et al.* [2008], among others, have showed how microphysical properties in different weather scenarios exhibit strong variability that depends on the storm type, e.g., they showed that stratiform events are dominated by small, slowly falling raindrops, while deep convective processes produce larger and faster falling raindrops. On the basis of the results of our study, the relationships between microphysics and weather types together with the relationships have shown between the rainfall cell statistics and the terminal velocity (or the originating DSD parameters) for different hydrometeors, can be invoked in order to enable the parameterization of physically based statistical downscaling models. In this respect, satellite-based observations of precipitating systems offer new opportunities for retrieval of microphysical properties of storms. For example, the active DPR, operating at Ku and Ka bands and planned to be board the core satellite of the GPM constellation [*Smith et al.*, 2007], is expected to provide information on the microphysical properties of precipitating systems over limited spatial extents (Figure 11). At the same time, the passive microwave products retrieved from the constellation of GPM satellites (GPM Microwave Imager, GMI) will be over larger a real extents but at resolutions of about 4.4–32 km (depending on the frequency), requiring thus downscaling down to scales of less than 1 km for hydrologic applications and hazard prediction. Defining a priori the parameters of such statistical downscaling schemes is difficult; however, this study presents a promising approach for relating these statistical downscaling parameters to small-scale microphysical parameters of the precipitating clouds. Incidently, these microphysical parameters are also explicitly used in the precipitation physical retrieval algorithms [e.g., *Masunaga and Kummerow*, 2005] providing thus the opportunity to more explicitly link retrieval and downscaling operations in real, or almost real time, and consistently over the footprint of both the DPR and GMI sensors. Such an approach would enable (1) a consistency between the GPM retrieved rainfall product and its downscaled version, (2) real-time downscaling capacity, and (3) the full use of ground validation

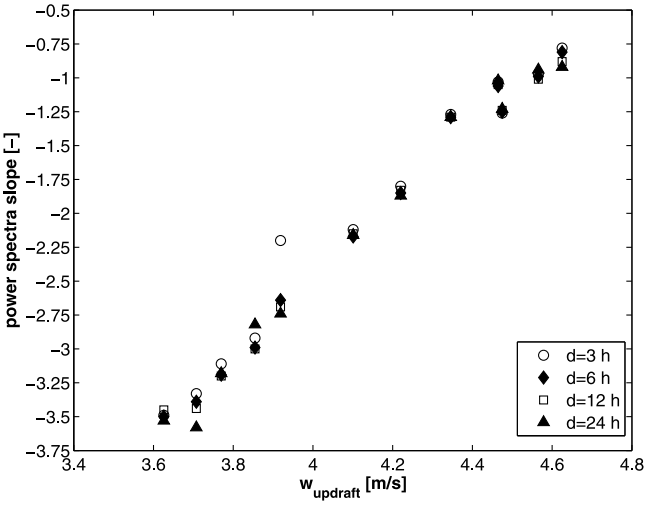

Figure 9. Accumulated rainfall (d = 3, 6, 12, and 24 h) spectral slope versus the updraft velocity scale w_{updraft} provided by *Parodi and Emanuel* [2009].

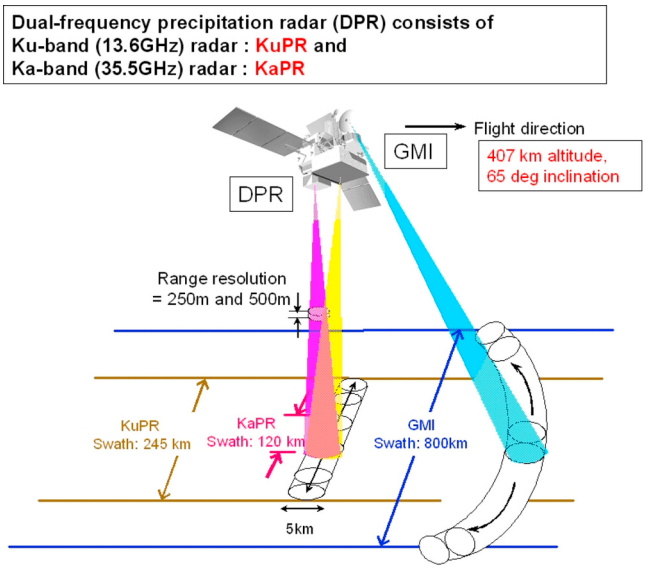

Figure 11. GPM sensors (GMI and DPR) (reproduced from http://gpm.gsfc.nasa.gov/dpr.html).

efforts toward both retrieval and downscaling. It is also interesting to note that in the future, Doppler Spaceborne Cloud and Precipitation Radars will be available to the community, thus the terminal velocity of precipitation will become a direct observable: a short list of instruments relevant to this point are the EarthCARE Doppler cloud profiling radar (European Space Agency (ESA)–JAXA), launch 2014) and the radar concepts proposed for the Polar Precipitation Mission (proposed to ESA within the Earth Explorer Opportunity Mission), and for the Aerosol/Clouds/Ecosystems mission (part of the NASA plan for the next decade). Until then, it will be necessary to define a solid approach, taking into account the associated uncertainties, that fully explores the retrieved particle size estimates which will be provided by DPR.

[24] A second direction of applications of the relationships established herein is that of providing independent information on parameterizing the conversion of radar reflectivity to rainfall intensity. Such a conversion could, for example, become conditional on, or constrained by, the drop size distribution inferred from the multiscale variability of the observed reflectivity (based on the relationships suggested in this study), noting that the scale-to-scale variability is preserved under the logarithmic transformation relating reflectivity to rainfall intensity.

7. Concluding Remarks

[25] The scope of this work was to examine, empirically and theoretically, how the multiscale variability of precipitation in deep moist convection can be quantified and concisely parameterized across space and time scales, and how this statistical parameterization can be related to physical observables. By using high-resolution simulations of an atmosphere in radiative-convective equilibrium performed with the WRF model, we attempted to provide a comprehensive picture of the role of raindrop terminal velocity in determining the multiscale statistical variability of the resulting precipitation fields. Specifically, we demonstrated that it is possible to adopt the raindrop terminal velocity as a physical parameter which explains to a large degree the statistical variability of convective rainfall over a range of scales. Our findings can be seen as a contribution to the challenge of relating the parameters of statistical downscaling schemes to microphysical or thermodynamic parameters of the storm environment for real-time or predictive downscaling, or for providing information on which precipitation retrieval from microwave sensors can be conditioned upon. Future work will be devoted to further exploring the theoretical and empirical evidence of these relationships in more realistic atmospheric scenarios, and to merging dual frequency radar information (for example from the active radar aboard the GPM core satellite) and other storm-environmental predictors (e.g., wind direction) for parameterizing the rainfall spatial variability at scales smaller than approximately the 4–10 km scale anticipated to be resolved by the passive microwave sensor of the GPM constellation of satellites.

Appendix A: Constant Raindrop Terminal Velocity V_T and DSD at Radiative-Convective Equilibrium

[26] Considering a DSD described by the Marshall-Palmer expression [*Marshall and Palmer*, 1948]

$$f_r(D) = N_0^r \exp(-\lambda_r D), \tag{A1}$$

where $N_0^r = 810^6\ m^{-4}$, the rainwater mixing ratio can be computed by

$$\rho q_r = N_0^r \int_0^\infty m(D) \exp(-\lambda_r D) dD, \tag{A2}$$

where the raindrop mass is $m(D) = \rho_w \pi\ (D^3/6)$, ρ is the air density, and ρ_w is the water density. Then we arrive at

$$\rho q_r = \pi \rho_w N_0^r \lambda_r^{-4}. \tag{A3}$$

The mean diameter $\bar{D}$ of the raindrops is then computed as

$$\bar{D} = \frac{2}{\lambda_r} = 2\left(\frac{\rho q_r}{\pi \rho_w N_0^r}\right)^{\frac{1}{4}}. \tag{A4}$$

For each numerical simulation, the mean value of ρq_r has been computed over the atmospheric layer (0–1000 m) only for convective pixels (where the vertical velocity $w > 2$ m/s [*Lemone*, 1983]). In this way the values of $\bar{D}$, for V_T in the range 1–5 m/s (exhibiting scaling behavior, see section 3.1) were computed (based on equation (A4), as a function of rainwater mixing ratio and air density) to be between 5×10^{-4} and 10^{-3} m, in reasonably good agreement with observations [*Pruppacher and Klett*, 1997; *Straka*, 2009]. This agreement places confidence that the terminal velocity values used in our simulations correspond to realistic DSDs in the precipitating clouds, and thus implies (by substituting λ_r from equation (A4) into equation (A1)) that in the numerical simulations the computed DSD (from the prescribed terminal velocities and the relevant equations) are within a physically reasonable range.

Appendix B: The Concept of Statistical Scaling

[27] In the context of this paper, we are interested to determine whether the probability distribution of rain cell sizes (A_C) can be renormalized with respect to the terminal velocity V_T (notice that V_T in our case serves as the "scale"). Simple scaling refers to the case where a simple renormalization involving only one parameter is possible, while multiscaling refers to the case in which more than one parameters are needed to collapse the probability density functions (PDFs) of A_c to each other for different values of V_T.

[28] Let us denote by $\langle A_C^q \rangle$ the qth statistical moment of A_c. For scaling to exist,

$$\langle A_C^q \rangle = \alpha_q V_T^{\tau(q)}, \tag{B1}$$

where α_q and $\tau(q)$ are functions of the order q of the statistical moment. If $\tau(q)$ is a linear function of q, i.e.,

$$\tau(q) = qh, \tag{B2}$$

then the process is called simple scaling and all statistical moments (and by extension the whole PDF of A_C) can be renormalized across different V_T values using the single parameter M. However, if $\tau(q)$ is a nonlinear function of q it means that statistical moments scale in a way that need more than one parameter to be renormalized (multiscaling). It can be easily shown from (12) that the coefficient of variation CV takes the form

$$\mathrm{CV}^2 = A V_T^{\tau(2)-2\tau(1)} - 1, \tag{B3}$$

where $A = \alpha_2/\alpha_1^2$. For a simple scaling process, $\tau(2) = 2\tau(1)$ and thus the CV is constant and independent of scale. However, for a multiscaling process, this is not the case. For example, the simplest nonlinear expression of $\tau(q)$ takes a quadratic form:

$$\tau(q) = c_1 q - \frac{c_2}{2} q^2. \tag{B4}$$

In this case, $\tau(2) - 2\tau(1) = c_1 - c_2$, and the CV takes the form

$$\mathrm{CV}^2 = A V_T^{c_1 - c_2} - 1, \tag{B5}$$

implying a dependence of CV on scale. Our results indicate the presence of simple scaling in the statistical structure of A_c for larger terminal velocities ($V_T > 6$ m s^{-1}) while for smaller velocities ($V_T < 5$ m s^{-1}), a multiscaling is present. In that multiscaling regime, $\tau(2) > 2\tau(1)$ implying that the variability of rain cell sizes increases proportionally faster than the mean rain cell size. This can be interpreted in the context that increased terminal velocity contributes to a richer hierarchical structure in precipitation intensities due to increased convective instability in the storm environment.

[29] **Acknowledgments.** The authors are grateful to F. Siccardi and S. Tanelli for enlightening discussions and useful comments. The comments of the anonymous reviewers and S. Lovejoy considerably improved our presentation. A.P. is grateful to the Italian Civil Protection Department for fundamental support of this research activity. E.F.-G. would like to acknowledge the support of a NASA-GPM grant (award NNX07AD33G) and of the National Center for Earth-Surface Dynamics, an NSF Science and Technology Center (award EAR-0120914).

References

Blossey, P., C. Bretherton, J. Cetrone, and M. Kharoutdinov (2007), Cloud-resolving model simulations of kwajex: Model sensitivities and comparisons with satellite and radar observations, *J. Atmos. Sci.*, *64*, 1488–1508.

Bradley, A., and J. Smith (1994), The hydrometeorological environment of extreme rainstorms in the southern plains of the United States, *J. Appl. Meteorol.*, *33*, 1418–1431.

Brawn, D., and G. Upton (2008), Estimation of an atmospheric gamma drop size distribution using disdrometer data, *Atmos. Res.*, *87*, 66–79.

Caracciolo, C., F. Prodi, A. Battaglia, and F. Porcu (2006), Analysis of the moments and parameters of a gamma DSD to infer precipitation properties: A convective stratiform discrimination algorithm, *Atmos. Res.*, *80*, 165–186.

Caracciolo, C., F. Porcu, and F. Prodi (2008), Precipitation classification at mid-latitudes in terms of drop size distribution parameters, *Adv. Geosci.*, *16*, 11–17.

Chumchean, S., S. Alan, and A. Sharma (2008), An operational approach for classifying storms in real-time radar rainfall estimation, *J. Hydrol.*, *363*, 1–17.

Cifelli, R., D. Rajopadhyaya, C. Williams, S. Avery, and P. May (2000), Drop size distribution characteristics in tropical mesoscale convective systems, *J. Appl. Meteorol.*, *39*, 760–767.

Emanuel, K. (1994), *Atmospheric Convection*, 580 pp., Oxford Univ. Press, New York.

Emanuel, K. A., and M. Bister (1996), Moist convective velocity and buoyancy scales, *J. Atmos. Sci.*, *53*, 3276–3285.

Feldman, D. R., T. S. L'Ecuyer, K. N. Liou, and Y. L. Yung (2008), Remote sensing of tropical tropopause layer radiation balance using A-train measurements, *J. Geophys. Res.*, *113*, D21113, doi:10.1029/2008JD010158.

Ferraris, L., S. Gabellani, U. Parodi, N. Rebora, J. von Hardenberg, and A. Provenzale (2003), Revisiting multifractality in rainfall fields, *J. Hydrometeorol.*, *4*, 544–551.

Frei, C., and C. Schar (1998), A precipitation climatology of the Alps from high-resolution rain-gauge observations, *Int. J. Climatol.*, *18*, 873–900.

Georgakakos, K. P., and J. Cramer (1994), Observation and analysis of midwestern rain rates, *J. Appl. Meteorol.*, *33*, 1433–1444.

Georgakakos, K. P., and W. F. Krajewski (1996), Statistical-microphysical causes of rainfall variability in the tropics, *J. Geophys. Res.*, *101*, 26,165–26,180, doi:10.1029/96JD01613.

Gilmore, M., J. Straka, and E. Rasmussen (2004), Precipitation uncertainty due to variations in precipitation particle parameters within a simple microphysics scheme, *Mon. Weather Rev.*, *132*, 2610–2627.

Grabowski, W. W. (2003), Impact of cloud microphysics on convective-radiative quasi equilibrium revealed by cloud-resolving convection parameterization, *J. Clim.*, *16*, 3463–3475.

Grubisic, V., R. Vellore, and A. Huggins (2005), Quantitative precipitation forecasting of wintertime storms in the Sierra Nevada: Sensitivity to the microphysical parameterization and horizontal resolution, *Mon. Weather Rev.*, *133*, 2834–2859.

Gryschka, M., B. Witha, and D. Etling (2008), Scale analysis of convective clouds, *Meteorol. Z.*, *17*, 785–791.

Gupta, V. K., and E. Waymire (1996), Multiplicative cascades and spatial variability in rainfall, river networks and floods, in *Reduction and Predictability of Natural Disasters*, pp. 71–96, Addison-Wesley, Boston, Mass.

Harris, D., E. Foufoula-Georgiou, K. Droegemeier, and J. Levit (2001), Multiscale statistical properties of a high-resolution precipitation forecast, *J. Hydrometeorol.*, *2*, 406–418.

Held, I. M., R. S. Hemler, and V. Ramaswamy (1993), Radiative-convective equilibrium with explicit two-dimensional moist convection, *J. Atmos. Sci.*, *50*, 3909–3927.

Hong, S., K. Sunny Lim, J. Kim, J. Jade Lim, and J. Dudhia (2009), Sensitivity study of cloud-resolving convective simulations with WRF using two bulk microphysical parameterizations: Ice-phase microphysics versus sedimentation effects, *J. Appl. Meteorol. Climatol.*, *48*, 61–76.

Islam, S., R. L. Bras, and K. Emanuel (1993), Predictability of mesoscale rainfall in the tropics, *J. Appl. Meteorol.*, *32*, 297–310.

Jordan, C. L. (1958), Mean soundings for the West Indies area, *J. Meteorol.*, *15*, 91–97.

Kessler, E. (1969), On the distribution and continuity of water substance in atmospheric circulation, *Meteorol. Monogr.*, *10*, 84 pp.

Kumar, P., and E. Foufoula-Georgiou (1993), A multicomponent decomposition of spatial rainfall fields: 1. Segregation of large and small scale features using wavelet transforms, *Water Resour. Res.*, *29*, 2515–2532, doi:10.1029/93WR00548.

Lemone, M. A. (1983), Momentum transport by a line of cumulonimbus, *J. Atmos. Sci.*, *40*, 1815–1834.

Liu, C., and M. Moncrieff (2007), Sensitivity of cloud-resolving simulations of warm-season convection to cloud microphysics parameterizations, *Mon. Weather Rev.*, *135*, 2854–2868.

Lovejoy, S. D., and V. C. Allaire (2008), The remarkable wide range spatial scaling of trmm precipitation, *Atmos. Res.*, *90*, 10–32.

Lovejoy, S., and D. Schertzer (1985), Generalized scale invariance in the atmosphere and fractal models of rain, *Water Resour. Res.*, *21*, 1233–1250, doi:10.1029/WR021i008p01233.

Lovejoy, S., and D. Scherzter (2006), Stereophotography of rain drops and compound Poisson-multifractal cascade processes, paper presented at the Cloud Physics Conference, Am. Meteorol. Soc., Madison, Wis.

Mandapaka, P. V., P. Lewandowski, W. E. Eichinger, and W. F. Krajewski (2009), Multiscaling analysis of high resolution space-time lidar-rainfall, *Nonlinear Process. Geophys.*, *16*, 579–586.

Marshall, J., and W. M. Palmer (1948), The distribution of raindrops with size, *J. Meteorol.*, *5*, 154–166.

Masunaga, H., and C. D. Kummerow (2005), Combined radar and radiometer analysis of precipitation profiles for a parametric retrieval algorithm, *J. Atmos. Oceanic Technol.*, *22*, 909–929.

Mellor, G. L., and T. Yamada (1974), A hierarchy of turbulence closure models for planetary boundary layers, *J. Atmos. Sci.*, *31*, 1791–1806.

Menabde, M., A. Seed, D. Harris, and G. Austin (1997), Self-similar random fields and rainfall simulation, *J. Geophys. Res.*, *102*, 13,509–13,515.

Molini, L., A. Parodi, and F. Siccardi (2009), Dealing with uncertainty: An analysis of the severe weather events over Italy in 2006, *Natl. Haz. Earth Syst. Sci.*, *9*, 1–13.

Nolan, D., E. Rappin, and K. Emanuel (2007), Tropical cyclogenesis sensitivity to environmental parameters in radiative convective equilibrium, *Q. J. R. Meteorol. Soc.*, *133*, 2085–2107.

Nykanen, D., and D. Harris (2003), Orographic influences on the multiscale statistical properties of precipitation, *J. Geophys. Res.*, *108*(D8), 8381, doi:10.1029/2001JD001518.

Olsson, N. J., and R. Berndtsson (1993), Fractal analysis of high-resolution rainfall time series, *J. Geophys. Res.*, *98*, 23,265–23,274, doi:10.1029/93JD02658.

Over, T., and V. Gupta (1994), Statistical analysis of mesoscale rainfall: Dependence of a random cascade generator on large-scale forcing, *J. Appl. Meteorol.*, *33*, 1526–1542.

Parodi, A., and K. Emanuel (2009), A theory for buoyancy and velocity scales in deep moist convection, *J. Atmos. Sci.*, *66*, 3449–3463.

Pauluis, O., and I. M. Held (2002a), Entropy budget of an atmosphere in radiative-convective equilibrium. Part I: Maximum work and frictional dissipation, *J. Atmos. Sci.*, *59*, 125–139.

Pauluis, O., and I. M. Held (2002b), Entropy budget of an atmosphere in radiative-convective equilibrium. Part II: Latent heat transport and moist processes, *J. Atmos. Sci.*, *59*, 140–149.

Perica, S., and E. Foufoula-Georgiou (1996), Linkage of scaling and thermodynamic parameters of rainfall: Results from midlatitude mesoscale convective systems, *J. Geophys. Res.*, *101*, 7431–7448, doi:10.1029/95JD02372.

Prandtl, L. (1910), Eine beziehung zwischen w armeustausch und str omungswiderstand der fl ussigkeiten, *Physik. Z.*, *XI*, 10721078.

Prandtl, L. (1925), Bericht uber untersuchungen zur ausgebildeten turubulenz, *Z. Angew. Math. Mech.*, *5*, 136–139.

Pruppacher, H. R., and J. D. Klett (1997), *Microphysics of Clouds and Precipitation*, Kluwer Acad., Norwell, Mass.

Robe, F. R., and K. Emanuel (1996), Moist convective scaling: Some inferences from three-dimensional cloud ensemble simulations, *J. Atmos. Sci.*, *53*, 3265–3275.

Robe, F. R., and K. Emanuel (2001), The effect of vertical wind shear on radiative-convective equilibrium states, *J. Atmos. Sci.*, *58*, 1427–1445.

Robin, J., A. Illingworth, and K. Halladay (2008), Estimating mass and momentum fluxes in a line of cumulonimbus using a single high-resolution Doppler radar, *Q. J. R. Meteorol. Soc.*, *64*, 1127–1141.

Rudari, R., D. Entekhabi, and G. Roth (2005), Large-scale atmospheric patterns associated with mesoscale features leading to extreme precipitation events in northwestern Italy, *Adv. Water Resour.*, *28*, 601–614.

Shutts, G. J., and M. E. B. Gray (2007), Numerical simulations of convective equilibrium under prescribed forcing, *Q. J. R. Meteorol. Soc.*, *125*, 2767–2787.

Skamarock, W. (2004), Evaluating mesoscale NWP models using kinetic energy spectra, *Mon. Weather Rev.*, *132*, 3019–3032.

Skamarock, W. C., J. B. Klemp, J. Dudhia, D. O. Gill, D. M. Barker, W. Wang, and J. G. Powers (2005), A description of the Advanced Research WRF Version 2, *NCAR TEch. Note, NCAR/TN-486+STR*, 88 pp.

Smith, E., et al. (2007), The international Global Precipitation Measurement (GPM) program and mission: An overview, in *Measuring Precipitation From Space: EURAINSAT and the Future*, edited by V. Levizzani and F. J. Turk, pp. 611–653, Kluwer Acad., Norwell, Mass.

Steiner, M., T. Yamada, R. Houze, and S. Yuter (1995), Climatological characterization of three-dimensional storm structure from operational radar and rain gauge data, *J. Appl. Meteorol.*, *34*, 1978–2007.

Straka, J. (2009), *Cloud and Precipitation Microphysics: Principles and Parameterizations*, Cambridge Univ. Press, New York.

Tao, W., et al. (2006), Retrieval of latent heating from TRMM measurements, *Bull. Am. Meteorol. Soc.*, *87*, 1555–1572.

Tompkins, A. M., and G. C. Craig (1998a), Radiative-convective equilibrium in a three-dimensional cloud ensemble models, *Q. J. R. Meteorol. Soc.*, *124*, 2073–2097.

Tompkins, A. M., and G. C. Craig (1998b), Sensitivity of tropical convection to sea surface temperature in the absence of large-scale flow, *J. Clim.*, *12*, 462–476.

Venugopal, V., and E. Foufoula-Georgiou (1996), Energy decomposition of rainfall in the time-frequency-scale domain using wavelet packets, *J. Hydrol.*, *187*, 3–27.

von Hardenberg, J., A. Provenzale, and A. Ferraris (2003), The shape of rain cells, *Geophys. Res. Lett.*, *30*(24), 2280, doi:10.1029/2003GL018539.

Vrac, M., and P. Yiou (2010), Weather regimes designed for local precipitation modeling: Application to the Mediterranean basin, *J. Geophys. Res.*, *115*, D12103, doi:10.1029/2009JD012871.

Waldvogel, A. (1974), The n_0 jump of raindrop spectra, *J. Atmos. Sci.*, *31*, 1067–1078.

Wu, W. (2002), Effects of ice microphysics on tropical radiative-convective-oceanic quasi-equilibrium states, *J. Atmos. Sci.*, *59*, 1885–1897.

Zawadski, I., E. Monteiro, and F. Fabry (1994), The development of drop size distributions in light rain, *J. Atmos. Sci.*, *51*, 1100–1113.

K. Emanuel, Program in Atmospheres, Oceans, and Climate, Massachusetts Institute of Technology, Rm. 54-1620, 77 Mass. Ave., Cambridge, MA 02139, USA.

E. Foufoula-Georgiou, Department of Civil Engineering, Saint Anthony Falls Laboratory, University of Minnesota, Minneapolis, MN 55414-2196, USA.

A. Parodi, CIMA Research Foundation, Via Magliotto 2, I-17100 Savona, Italy. (antonio.parodi@cimafoundation.org)